

Lattice QCD Calculation of the ρ Meson Decay Width

S. Aoki,^{1,2} M. Fukugita,³ K-I. Ishikawa,⁴ N. Ishizuka,^{1,5} K. Kanaya,¹ Y. Kuramashi,^{1,5}
Y. Namekawa,^{6,*} M. Okawa,⁴ K. Sasaki,⁵ A. Ukawa,^{1,5} and T. Yoshié^{1,5}

(CP-PACS Collaboration)

¹ *Graduate School of Pure and Applied Sciences,
University of Tsukuba, Tsukuba, Ibaraki 305-8571, Japan*

² *Riken BNL Research Center, Brookhaven
National Laboratory, Upton, New York 11973, USA*

³ *Institute for Cosmic Ray Research,
University of Tokyo, Kashiwa 277 8582, Japan*

⁴ *Department of Physics, Hiroshima University,
Higashi-Hiroshima, Hiroshima 739-8526, Japan*

⁵ *Center for Computational Sciences,
University of Tsukuba, Tsukuba, Ibaraki 305-8577, Japan*

⁶ *Department of Physics, Nagoya University, Nagoya 464-8602, Japan*

(Dated: October 27, 2018)

Abstract

We present a lattice QCD calculation of the ρ meson decay width via the P -wave scattering phase shift for the $I = 1$ two-pion system. Our calculation uses full QCD gauge configurations for $N_f = 2$ flavors generated using a renormalization group improved gauge action and an improved Wilson fermion action on a $12^3 \times 24$ lattice at $m_\pi/m_\rho = 0.41$ and the lattice spacing $1/a = 0.92$ GeV. The phase shift calculated with the use of the finite size formula for the two-pion system in the moving frame shows a behavior consistent with the existence of a resonance at a mass close to the vector meson mass obtained in spectroscopy. The decay width estimated from the phase shift is consistent with the experiment, when the quark mass is scaled to the realistic value.

PACS numbers: 12.38.Gc, 11.15.Ha

*Present address : Center for Computational Sciences, University of Tsukuba, Tsukuba, Ibaraki 305-8577, Japan

I. INTRODUCTION

A study of the ρ meson decay is a significant step for understanding the dynamical aspect of hadron reactions with lattice QCD. We notice three studies carried out to date toward this direction. The earlier two [1, 2] employed the quenched approximation ignoring the decay into two ghost pions which appear in the quenched theory. The third one used the full QCD [3] and estimated the decay width from the $\rho \rightarrow \pi\pi$ transition amplitude $\langle \rho | \pi\pi \rangle$ extracted from the time behavior of the correlation functions $\langle 0 | \pi(t)\pi(t)\rho(0) | 0 \rangle$ and $\langle 0 | \pi(t)\pi(t)\pi(0)\pi(0) | 0 \rangle$, assuming that the hadron interaction is small. These studies, however, were all carried out at unphysical kinematics $m_\pi/m_\rho > 1/2$.

In the present work we attempt to carry out a more realistic calculation. We estimate the ρ meson decay width by calculating the P -wave scattering phase shift for the $I = 1$ two-pion system. The calculations are carried out with $N_f = 2$ full QCD configurations previously generated for a study of the light hadron spectrum with a renormalization group improved gauge action and a clover fermion action at $\beta = 1.8$, $\kappa = 0.14705$ on a $12^3 \times 24$ lattice [5]. The lattice parameters were determined from the spectrum analysis which gave $m_\pi/m_\rho = 0.41$, the lattice extent $L = 2.53$ fm and the lattice space inverse $1/a = 0.92$ GeV. The finite size formula presented by Rummukainen and Gottlieb [4] is employed to estimate the phase shift. This calculation is made at two energies that allow to study the existence of the resonance.

This paper is organized as follows. In Sec. II we give the method of the calculations and the simulation parameters. We present our results in Sec. III. Our conclusions are given in Sec. IV. Preliminary reports of the present work were presented in [6]. The calculation was carried out on VPP5000/80 at the Academic Computing and Communications Center of University of Tsukuba.

II. METHODS

A. Rummukainen-Gottlieb formula

Let us consider the ρ meson decay into the two pions in the P -wave. When the ρ meson is at rest, the energy of the two pions, neglecting the final state interaction, is

$$E = 2\sqrt{m_\pi^2 + p^2}, \quad (1)$$

where the momentum takes $\mathbf{p} = (2\pi/L)\mathbf{n}$ ($\mathbf{n} \in \mathbb{Z}^3 \neq 0$) on the lattice. In a typical full QCD simulation on $L \sim 2 - 3$ fm, this energy is significantly larger than the resonance mass m_ρ . On our full QCD configurations, for example, the lowest energy estimated from m_π and m_ρ calculated in the previous study [5] is $E = 1.47 \times m_\rho$, appreciably away from the resonance and it is not suitable to study the ρ meson decay.

In order to realize the kinematics such that the energy of the two pions is close to m_ρ , we consider a system having a non-zero total momentum, *i.e.*, the moving frame [4], with the total momentum $\mathbf{p} = p\mathbf{e}_3 = (2\pi/L)\mathbf{e}_3$ in a box satisfying the L^3 periodic boundary

condition. We set the system to the \mathbf{A}_2^- representation of the rotation group on the lattice (the tetragonal rotation group D_{4h}), which represents the $J = 1$ spin state ignoring effects from higher spin states with $J \geq 3$. We consider the iso-spin representation of $(I, I_z) = (1, 0)$, the neutral ρ meson.

For non-interacting hadrons the dominant low energy states in the moving frame are the two free pions with the momenta \mathbf{p} and $\mathbf{0}$, and the ρ meson with the momentum \mathbf{p} and a polarization vector parallel to the momentum, $\rho_3(\mathbf{p})$. The energies of these states are

$$\begin{aligned} W_1^0 &= \sqrt{m_\pi^2 + p^2} + m_\pi && \text{for the two free pions} \quad , \\ W_2^0 &= \sqrt{m_\rho^2 + p^2} && \text{for the } \rho \text{ meson} \quad . \end{aligned} \quad (2)$$

Other states having higher energies are neglected. On our full QCD configurations the invariant mass of the two free pions takes $\sqrt{s} = 0.97 \times m_\rho$, which is closer to m_ρ than that given by (1) for the system having the zero total momentum.

The hadron interaction shifts the energy from W_n^0 to W_n ($n = 1, 2$), and the energies W_n are related to the two-pion scattering phase shift δ in the infinite volume through the Rummukainen-Gottlieb formula [4], which is an extension of the Lüscher formula [7] to the moving frame. The formula for the \mathbf{A}_2^- representation and the total momentum $\mathbf{p} = p\mathbf{e}_3$ reads

$$\frac{1}{\tan \delta} = Z(1; kL/(2\pi)) \quad , \quad (3)$$

where k is the momentum defined from the invariant mass \sqrt{s} as $\sqrt{s} = \sqrt{W^2 - p^2} = 2\sqrt{k^2 + m_\pi^2}$. The function Z is an analytic continuation of

$$Z(x; q) = \frac{1}{2\pi^2 q \gamma} \sum_{\mathbf{r} \in \Gamma} \frac{1 + (3r_3^2 - r^2)/q^2}{(r^2 - q^2)^x} \quad , \quad (4)$$

which is defined for $\text{Re}(x) > 5/2$, where $\gamma = W/\sqrt{s}$ is the Lorentz boost factor and the summation for \mathbf{r} runs over the set

$$\Gamma = \left\{ \mathbf{r} \mid r_1 = n_1 \quad , \quad r_2 = n_2 \quad , \quad r_3 = \left(n_3 + \frac{pL}{2\pi} \right) / \gamma \quad , \quad \mathbf{n} \in \mathbb{Z}^3 \right\} \quad . \quad (5)$$

$Z(1; q)$ can be evaluated by the method described in Ref. [8].

B. Extraction of energies

In order to calculate the two energies W_n ($n = 1, 2$) we construct a matrix of the time correlation function,

$$G(t) = \begin{pmatrix} \langle 0 | (\pi\pi)^\dagger(t) (\pi\pi)(t_S) | 0 \rangle & \langle 0 | (\pi\pi)^\dagger(t) \rho_3(t_S) | 0 \rangle \\ \langle 0 | \rho_3^\dagger(t) (\pi\pi)(t_S) | 0 \rangle & \langle 0 | \rho_3^\dagger(t) \rho_3(t_S) | 0 \rangle \end{pmatrix} \quad , \quad (6)$$

where $\rho_3(t)$ is an interpolating operator for the neutral ρ meson with the momentum $\mathbf{p} = (2\pi/L)\mathbf{e}_3$ and the polarization vector parallel to \mathbf{p} , and $(\pi\pi)(t)$ is an interpolating operator

for the two free pions,

$$(\pi\pi)(t) = \frac{1}{\sqrt{2}} \left(\pi^-(\mathbf{p}, t) \pi^+(\mathbf{0}, t) - \pi^+(\mathbf{p}, t) \pi^-(\mathbf{0}, t) \right). \quad (7)$$

These operators belong to the \mathbf{A}_2^- and the $(I, I_z) = (1, 0)$.

To extract W_n ($n = 1, 2$) we construct a matrix,

$$M(t, t_R) = G(t) G^{-1}(t_R), \quad (8)$$

with some reference time t_R [9]. The two eigenvalues $\lambda_n(t, t_R)$ ($n = 1, 2$) of the matrix $M(t, t_R)$ behave as

$$\lambda_n(t, t_R) = e^{-W_n \cdot (t - t_R)}, \quad (9)$$

for a large t , if the two lowest states dominate the correlation function. The two energies W_n can be extracted by a single exponential fit to $\lambda_n(t, t_R)$.

In order to construct the meson state with a non-zero momentum we introduce $U(1)$ noise $\xi_j(\mathbf{x})$ in three-dimensional space, which satisfies

$$\sum_{j=1}^{N_R} \xi_j^*(\mathbf{x}) \xi_j(\mathbf{y}) = \delta^3(\mathbf{x} - \mathbf{y}) \quad \text{for } N_R \rightarrow \infty, \quad (10)$$

where N_R is the number of the noise representation taken to be 10 in the present work. We calculate the quark propagator,

$$Q_{AB}(\mathbf{x}, t | \mathbf{q}, t_S, \xi_j) = \sum_{\mathbf{y}} (D^{-1})_{AB}(\mathbf{x}, t; \mathbf{y}, t_S) \cdot \left[e^{i\mathbf{q} \cdot \mathbf{y}} \xi_j(\mathbf{y}) \right], \quad (11)$$

where A and B refer to color and spin indices. The square bracket in (11) is taken as the source term in solving the propagator. The two point function of the meson with the spin content Γ and the momentum \mathbf{p} can be constructed from Q by

$$\sum_{j=1}^{N_R} \sum_{\mathbf{x}} e^{-i\mathbf{p} \cdot \mathbf{x}} \left\langle \gamma_5 Q^\dagger(\mathbf{x}, t | \mathbf{0}, t_S, \xi_j) \gamma_5 \Gamma^\dagger Q(\mathbf{x}, t | \mathbf{p}, t_S, \xi_j) \Gamma \right\rangle, \quad (12)$$

where the bracket means the trace with respect to the color and the spin indices; hereafter we take this convention for the brackets.

The contractions of the quark field for the components of $G(t)$ are shown in Fig. 1. The vertices refer to the pion or the ρ meson with the momentum specified in the diagrams. The time runs upward in the diagrams. The function $G_{\pi\pi \rightarrow \pi\pi}(t)$ for the first diagram in Fig. 1 is calculated by introducing in addition another $U(1)$ noise $\eta_j(\mathbf{x})$ having the property identical to that of $\xi_j(\mathbf{x})$ as in (10),

$$G_{\pi\pi \rightarrow \pi\pi}^{[1st]} = \sum_{j=1}^{N_R} \sum_{\mathbf{x}, \mathbf{y}} e^{-i\mathbf{p} \cdot \mathbf{x}} \left\langle Q^\dagger(\mathbf{x}, t | \mathbf{0}, t_S, \xi_j) Q(\mathbf{x}, t | \mathbf{p}, t_S, \xi_j) \right\rangle \left\langle Q^\dagger(\mathbf{y}, t | \mathbf{0}, t_S, \eta_j) Q(\mathbf{y}, t | \mathbf{0}, t_S, \eta_j) \right\rangle. \quad (13)$$

The function $G_{\pi\pi\rightarrow\pi\pi}(t)$ for the second diagram is obtained by exchanging the momenta of the sink in (13).

To obtain the $G(t)$ for the other diagrams we calculate the quark propagator of a different type by the source method,

$$W_{AB}(\mathbf{x}, t | \mathbf{k}, t_1 | \mathbf{q}, t_S, \xi_j) = \sum_{\mathbf{z}} \sum_C (D^{-1})_{AC}(\mathbf{x}, t; \mathbf{z}, t_1) \cdot \left[e^{i\mathbf{k}\cdot\mathbf{z}} \gamma_5 Q(\mathbf{z}, t_1 | \mathbf{q}, t_S, \xi_j) \right]_{CB}, \quad (14)$$

where A , B and C refer to color and spin indices, and the term in the square bracket is taken as the source term in solving the propagator. Using W we calculate the functions $G_{\pi\pi\rightarrow\pi\pi}(t)$ for the third to sixth diagrams in Fig. 1 by

$$\begin{aligned} G_{\pi\pi\rightarrow\pi\pi}^{[3rd]} &= \sum_{j=1}^{N_R} \sum_{\mathbf{x}} e^{-i\mathbf{p}\cdot\mathbf{x}} \left\langle W^\dagger(\mathbf{x}, t | \mathbf{0}, t_S | -\mathbf{p}, t_S, \xi_j) W(\mathbf{x}, t | \mathbf{0}, t | \mathbf{0}, t_S, \xi_j) \right\rangle, \\ G_{\pi\pi\rightarrow\pi\pi}^{[4th]} &= \sum_{j=1}^{N_R} \sum_{\mathbf{x}} e^{-i\mathbf{p}\cdot\mathbf{x}} \left\langle W(\mathbf{x}, t | \mathbf{0}, t_S | \mathbf{p}, t_S, \xi_j) W^\dagger(\mathbf{x}, t | \mathbf{0}, t | \mathbf{0}, t_S, \xi_j) \right\rangle, \\ G_{\pi\pi\rightarrow\pi\pi}^{[5th]} &= \sum_{j=1}^{N_R} \sum_{\mathbf{x}} e^{-i\mathbf{p}\cdot\mathbf{x}} \left\langle W(\mathbf{x}, t | \mathbf{p}, t_S | \mathbf{0}, t_S, \xi_j) W^\dagger(\mathbf{x}, t | \mathbf{0}, t | \mathbf{0}, t_S, \xi_j) \right\rangle, \\ G_{\pi\pi\rightarrow\pi\pi}^{[6th]} &= \sum_{j=1}^{N_R} \sum_{\mathbf{x}} e^{-i\mathbf{p}\cdot\mathbf{x}} \left\langle W^\dagger(\mathbf{x}, t | -\mathbf{p}, t_S | \mathbf{0}, t_S, \xi_j) W(\mathbf{x}, t | \mathbf{0}, t | \mathbf{0}, t_S, \xi_j) \right\rangle. \end{aligned} \quad (15)$$

The functions $G_{\pi\pi\rightarrow\rho}(t)$ for the two diagrams in Fig. 1 can be calculated by

$$\begin{aligned} G_{\pi\pi\rightarrow\rho}^{[1st]} &= \sum_{j=1}^{N_R} \sum_{\mathbf{x}} e^{-i\mathbf{p}\cdot\mathbf{x}} \left\langle Q(\mathbf{x}, t | \mathbf{0}, t_S, \xi_j) W^\dagger(\mathbf{x}, t | -\mathbf{p}, t_S | \mathbf{0}, t_S, \xi_j) \gamma_5 \gamma_3 \right\rangle, \\ G_{\pi\pi\rightarrow\rho}^{[2nd]} &= \sum_{j=1}^{N_R} \sum_{\mathbf{x}} e^{-i\mathbf{p}\cdot\mathbf{x}} \left\langle W(\mathbf{x}, t | \mathbf{p}, t_S | \mathbf{0}, t_S, \xi_j) Q^\dagger(\mathbf{x}, t | \mathbf{0}, t_S, \xi_j) \gamma_5 \gamma_3 \right\rangle, \end{aligned} \quad (16)$$

and similarly for $G_{\rho\rightarrow\pi\pi}(t)$,

$$\begin{aligned} G_{\rho\rightarrow\pi\pi}^{[1st]} &= - \sum_{j=1}^{N_R} \sum_{\mathbf{x}} e^{-i\mathbf{p}\cdot\mathbf{x}} \left\langle W^\dagger(\mathbf{x}, t | \mathbf{0}, t | \mathbf{0}, t_S, \xi_j) Q(\mathbf{x}, t | \mathbf{p}, t_S, \xi_j) \gamma_5 \gamma_3 \right\rangle, \\ G_{\rho\rightarrow\pi\pi}^{[2nd]} &= - \sum_{j=1}^{N_R} \sum_{\mathbf{x}} e^{-i\mathbf{p}\cdot\mathbf{x}} \left\langle Q^\dagger(\mathbf{x}, t | -\mathbf{p}, t_S, \xi_j) W(\mathbf{x}, t | \mathbf{0}, t | \mathbf{0}, t_S, \xi_j) \gamma_5 \gamma_3 \right\rangle. \end{aligned} \quad (17)$$

The quark propagators are solved with the Dirichlet boundary condition imposed in the time direction and the source operator is set at $t_S = 4$ which is sufficiently large to avoid effects from the temporal boundary. We calculate the Q -type propagators (11) for four sets of \mathbf{q} and the $U(1)$ noise:

$$(\mathbf{q}, \text{noise}) = \{ (\mathbf{0}, \xi), (\mathbf{0}, \eta), (\mathbf{p}, \xi), (-\mathbf{p}, \xi) \}. \quad (18)$$

The W -type propagators (14) are calculated for 22 sets of \mathbf{k} , t_1 and \mathbf{q} :

$$(\mathbf{k}, t_1 | \mathbf{q}) = \{ (\mathbf{p}, t_S | \mathbf{0}), (-\mathbf{p}, t_S | \mathbf{0}), (\mathbf{0}, t_S | \mathbf{p}), (\mathbf{0}, t_S | -\mathbf{p}), (\mathbf{0}, t_1 = 4 - 21 | \mathbf{0}) \}, \quad (19)$$

using the same $U(1)$ noise representation ξ in common. All time correlation functions can be calculated with combinations of these propagators. We carry out additional measurements to reduce statistical errors using the source operator located at $t_S + T/2$ with the Dirichlet boundary condition at $T/2$, and average over the two measurements. Thus we calculate $(4 + 22) \times 10 \times 2 = 520$ quark propagators for each configuration.

C. Simulation parameters

Calculations employ $N_f = 2$ full QCD configurations previously generated for a study of the light hadron spectrum using a renormalization group improved gauge action and a clover fermion action at $\beta = 1.8$, $\kappa = 0.14705$ with the mean-field improvement taking $C_{SW} = 1.60$ on a $12^3 \times 24$ lattice [5]. The periodic boundary conditions are imposed for both spatial and temporal directions in configuration generations and the Dirichlet boundary condition for the temporal direction in calculations of quark propagators. The lattice parameters determined from the spectrum analysis are $m_\pi/m_\rho = 0.41$, $L = 2.53$ fm and $1/a = 0.92$ GeV. The total number of configurations analyzed every 5 trajectories is 800. We estimate the statistical errors by the jackknife method with bins of 100 trajectories.

III. RESULTS

A. Time correlation function

In Fig. 2 we show the real part of the diagonal components ($\pi\pi \rightarrow \pi\pi$ and $\rho \rightarrow \rho$) and the imaginary part of the off-diagonal components ($\pi\pi \rightarrow \rho$ and $\rho \rightarrow \pi\pi$) of the time correlation function $G(t)$ in (6). $G(t)$ is a Hermitian matrix, since the sink and source operators are identical for a sufficiently large N_R or equivalently for a large number of configurations. The off-diagonal components are pure imaginary by P and CP symmetry. We find that these hold true within statistics. The $\rho \rightarrow \pi\pi$ component agrees with $\pi\pi \rightarrow \rho$ as seen in Fig. 2 within the error, but the statistical errors of the former is large for a large t . Hence, in the following analysis we substitute $\rho \rightarrow \pi\pi$ by $\pi\pi \rightarrow \rho$ to reduce errors.

We calculate the two eigenvalues $\lambda_n(t, t_R)$ ($n = 1, 2$) for the matrix $M(t, t_R)$ in (8) with the reference time $t_R = 9$. In Fig. 3 we plot the normalized eigenvalues $R_n(t, t_R)$ ($n = 1, 2$) defined by

$$R_n(t, t_R) = \lambda_n(t, t_R) \frac{G_\pi(t_R; \mathbf{p}) G_\pi(t_R; \mathbf{0})}{G_\pi(t; \mathbf{p}) G_\pi(t; \mathbf{0})}, \quad (20)$$

where $G_\pi(t; \mathbf{p})$ is the time correlation function for the pion with the momentum \mathbf{p} ,

$$G_\pi(t; \mathbf{p}) = \langle 0 | \pi^\dagger(\mathbf{p}, t) \pi(\mathbf{p}, t_S) | 0 \rangle. \quad (21)$$

The slope of the curves in Fig. 3 represents the energy difference with respect to the energy of the two free pions, *i.e.*, $\Delta W_n = W_n - W_1^0$. We observe that the energy difference for $R_1(t, t_R)$ is negative and that for $R_2(t, t_R)$ positive, meaning that the phase shift is positive and negative, respectively, consistent with the presence of a resonance in between.

We extract the energy difference ΔW_n for both states by a single exponential fit to $R_n(t, t_R)$ for the time range $t = 10 - 16$. The energy of the two free pions W_1^0 is calculated from the mass m_π and the energy E obtained by a single exponential fit to $G_\pi(t; \mathbf{0})$ and $G_\pi(t; \mathbf{p})$ in (21), as $W_1^0 = m_\pi + E$. The energy W_n is reconstructed by $W_n = \Delta W_n + W_1^0$. The results are tabulated in the upper part of Table I.

B. Effect of finite lattice spacing

To see the size of errors arising from the discretization of the energy and the momentum on the lattice, we study the accuracy of the dispersion relation for the single particle. In the upper part of Table II we show the mass m and the energy E of the pion and the ρ meson with the momentum $\mathbf{p} = (2\pi/L)\mathbf{e}_3$, calculated from the time correlation functions. The ρ meson with zero momentum $\rho_j(\mathbf{0})$ ($j = 1, 2, 3$) and that having the momentum with the perpendicular polarization $\rho_j(\mathbf{p})$ ($j = 1, 2$) cannot decay energetically, so that the mass and the energy are obtained from the time correlation functions in a usual way.

In the continuum we have a relation

$$E = \sqrt{p^2 + m^2} , \quad (22)$$

for the single particle. We expect that the relation is modified on the lattice to

$$\cosh(E) = 2 \cdot \sin^2(p/2) + \cosh(m) . \quad (23)$$

For the measured m and E we calculate the momenta p_{eff} from the two dispersion relations (22) and (23). We expect that these p_{eff} agree with the pre-set momentum $p = 2\pi/L$ up to the discretization error. The lower part of Table II shows p_{eff} and the ratio p_{eff}^2/p^2 whose departure from unity is a measure for the violation of the dispersion relation due to the discretization error. We find that the relation on the lattice (23) satisfies well, whereas that in the continuum (22) does not hold so well for the pion. For the ρ meson the departure from unity is not clearly detected due to a large statistical error.

We should also be concerned with the discretization error for the two-pion system. We may think of two sources of the errors in the Rummukainen-Gottlieb formula (3). One of them arises from the Lorentz transformation from the moving frame to the center of mass frame using Lorentz symmetry in the continuum. In the transformation we use the relations,

$$\begin{aligned} \sqrt{s} &= \sqrt{W^2 - p^2} , \\ k^2 &= s/4 - m_\pi^2 , \end{aligned} \quad (24)$$

for the invariant mass \sqrt{s} , the energy in the moving frame W and the momentum k . These relations suffer from the discretization error, and hence the definitions of \sqrt{s} and k contain similar errors.

After the Lorentz transformation we obtain the Helmholtz equation for the two-pion wave function $\phi(\mathbf{x})$ in the center of mass frame,

$$\left(\nabla^2 + k^2\right)\phi(\mathbf{x}) = 0 \quad \text{for } |\vec{x}| > R, \quad (25)$$

where R is the two-pion interaction range. In Ref. [4] Rummukainen and Gottlieb derived the formula by solving (25) ignoring the effect of the finite lattice spacing. Thus the discretization error also appears here.

The violation of the dispersion relation in the continuum (22) has also been shown in Ref. [4], where the phase shift for the S -wave state was calculated for a statistical model. Motivated from the validity of the dispersion relation on the lattice (23), Rummukainen and Gottlieb obtained the invariant mass \sqrt{s} and the momentum k from the energy in the moving frame W as

$$\begin{aligned} \cosh(\sqrt{s}) &= \cosh(W) - 2 \cdot \sin^2(p/2), \\ 2 \cdot \sin^2(k/2) &= \cosh(\sqrt{s}/2) - \cosh(m_\pi), \end{aligned} \quad (26)$$

and the phase shift was obtained by substituting k into their formula. The discretization error arising in solving (25), however, was not worked out.

In the present work we calculate the invariant mass \sqrt{s} and the momentum k from the energy-momentum relations both in the continuum (24) and on the lattice (26), and estimate the phase shift by putting k into (3). We take the difference arising from the two choices as the discretization error. It is expected that this error vanishes in the continuum limit.

C. Scattering phase shift and decay width

The invariant mass \sqrt{s} , the momentum k and the phase shift δ obtained by the procedure in the previous subsection are presented in the lower part of Table I. Appreciable differences that depend on the energy-momentum relations used are visible in \sqrt{s} and k , but the difference for δ is comparable with statistical errors. These are also shown in the lower panel of Fig. 4, where the phase shift $\sin^2 \delta$, which is proportional to the scattering cross section of the two-pion system, is plotted. In Table I we see that the sign of δ at $\sqrt{s} < m_\rho$ ($m_\rho = 0.858 \pm 0.012$) is positive (attractive interaction) and that at $\sqrt{s} > m_\rho$ is negative (repulsive interaction) as expected. This confirms the existence of a resonance at a mass around m_ρ .

It may in principle be a straightforward task to estimate the ρ meson decay width by fitting the phase shift data with the Breit-Wigner formula. The quark mass we worked with, however, is much heavier than the realistic value, so that a long extrapolation is needed. Since we expect kinematic factors in the decay width depend largely on the quark mass while we made a simulation for only one set of the quark mass, we avoid this direct measurement of the decay width and take a different approach. We parametrize the resonant behavior of the P -wave phase shift in terms of the effective $\rho \rightarrow \pi\pi$ coupling constant $g_{\rho\pi\pi}$ as

$$\tan \delta = \frac{g_{\rho\pi\pi}^2}{6\pi} \frac{k^3}{\sqrt{s}(M_R^2 - s)}, \quad (27)$$

as in the continuum theory, where M_R is the resonance mass and $g_{\rho\pi\pi}$ is defined by

$$L_{\text{eff}} = g_{\rho\pi\pi} \sum_{abc} \epsilon_{abc} (k_1 - k_2)_\mu \rho_\mu^a(p) \pi^b(k_1) \pi^c(k_2) . \quad (28)$$

We may expect that such a coupling constant does not vary too rapidly as the quark mass changes.

In (27) the invariant mass \sqrt{s} and the momentum k that appear in the effective theory in the continuum satisfy the energy-momentum relations in the continuum (24). A further discretization error may then appear in the definition of \sqrt{s} and k upon the application of (27) to the phase shift calculated on the lattice. We find, however, that this does not lead numerically to a serious error. In Table I we give the momentum $k_0^2 = s/4 - m_\pi^2$ calculated from \sqrt{s} , and show that the difference between k and k_0 is small. Thus the error caused by the different definitions of the momentum is negligible. We adopt k_0 in the application of (27).

The results of the coupling $g_{\rho\pi\pi}$ and the resonance mass M_R given by (27) are

$$\begin{aligned} g_{\rho\pi\pi} &= 6.25 \pm 0.67 \\ M_R &= 0.851 \pm 0.024 \\ M_R/m_\rho &= 0.992 \pm 0.033 \end{aligned} \quad (29)$$

using the energy-momentum relations in the continuum (24), and

$$\begin{aligned} g_{\rho\pi\pi} &= 5.82 \pm 0.55 \\ M_R &= 0.906 \pm 0.028 \\ M_R/m_\rho &= 1.056 \pm 0.038 \end{aligned} \quad (30)$$

using those on the lattice (26), where m_ρ is the ρ meson mass extracted from the time correlation function in the previous section. In the lower panel of Fig. 4 we draw the curve for $\sin^2 \delta$ given by (27) with $g_{\rho\pi\pi}$ and M_R given in (29) and (30). The position at $\sin^2 \delta = 1$ that corresponds to the resonance mass M_R is also plotted in the upper panel of Fig. 4 for the two cases and compared with m_ρ . We find that M_R is consistent with m_ρ .

Assuming that the dependence of $g_{\rho\pi\pi}$ on quark mass is small, we estimate the ρ meson decay width at the physical quark mass as

$$\Gamma^{\text{ph}} = \frac{g_{\rho\pi\pi}^2}{6\pi} \frac{(k^{\text{ph}})^3}{(m_\rho^{\text{ph}})^2} = g_{\rho\pi\pi}^2 \times 4.128 \text{ MeV} , \quad (31)$$

where $m_\rho^{\text{ph}} = 770 \text{ MeV}$ is the actual ρ meson mass and $(k^{\text{ph}})^2 = (m_\rho^{\text{ph}})^2/4 - (m_\pi^{\text{ph}})^2$ ($m_\pi^{\text{ph}} = 140 \text{ MeV}$). This yields

$$\Gamma^{\text{ph}} = 162 \pm 35 \text{ MeV} \quad (32)$$

for (29), and

$$\Gamma^{\text{ph}} = 140 \pm 27 \text{ MeV} \quad (33)$$

for (30). These estimates are consistent with experiment, $\Gamma = 150 \text{ MeV}$. The difference that arises from the two energy-momentum relations used is comparable with the statistical

error. This is an encouraging result, although we assumed that the coupling constant does not depend on the quark mass to make a long extrapolation and we did not trace the propagation of discretization errors that appear in various steps so accurately.

IV. CONCLUSIONS

We have shown that a calculation of the P -wave scattering phase shift for the $I = 1$ two-pion system and estimation of the decay width therefrom are feasible on the lattice with present computing resources. The phase shift data shows the existence of a resonance at a mass close to the vector meson mass obtained in the spectroscopy. This resonance can certainly be identified with the ρ meson. We extracted the ρ meson decay width from the phase shift data and showed that it is consistent with the experiment.

We note, however, at the same time several important issues that should be cleared in the future work. One of the important issues is to reduce the discretization error in the kinematic relations among the invariant mass \sqrt{s} , the energy in the moving frame W and the momentum k on the lattice, needed to evaluate the phase shift. An obvious way to solve this problem is to use a lattice closer to the continuum limit.

We have used the effective $\rho \rightarrow \pi\pi$ coupling constant $g_{\rho\pi\pi}$ to extrapolate from the point $m_\pi/m_\rho = 0.41$, where our simulation is made, to the physical point $m_\pi/m_\rho = 0.18$, assuming that $g_{\rho\pi\pi}$ does not depend on the quark mass. More direct evaluation of the decay width is clearly desirable. The decay width may be estimated directly from the energy dependence of the phase shift data by fitting the Breit-Wigner resonance formula, if the simulations are made close to the physical quark mass and we have data for several energy near the resonance mass. We must leave these issues to studies in the future.

Acknowledgments

This work is supported in part by Grants-in-Aid of the Ministry of Education (Nos. 13135204, 13135216, 15540251, 16540228, 16740147, 17340066, 17540259, 18104005, 18540250, 18740139). The numerical calculations have been carried out on VPP5000/80 at Academic Computing and Communications Center of University of Tsukuba.

-
- [1] S. Gottlieb, P.B. Mackenzie, H.B. Thacker, and D. Weingarten, Phys. Lett. **B134** (1984) 346.
 - [2] R.D. Loft and T.A. DeGrand, Phys. Rev. **D39** (1989) 2692.
 - [3] UKQCD Collaboration, C. McNeile and C. Michael, Phys. Lett. **B556** (2003) 177.
 - [4] K. Rummukainen and S. Gottlieb, Nucl. Phys. **B450** (1995) 397.
 - [5] CP-PACS Collaboration, Y. Namekawa *et al.*, Phys. Rev. **D70** (2004) 074503.
 - [6] CP-PACS Collaboration, S. Aoki *et al.*, Proc. Sci. LAT2006 (2006) 110; hep-lat/0610020.
 - [7] M. Lüscher, Commun. Math. Phys. **105** (1986) 153; Nucl. Phys. **B354** (1991) 531.
 - [8] CP-PACS Collaboration, T. Yamazaki *et al.*, Phys. Rev. **D70** (2004) 074513.

[9] M. Lüscher and U. Wolff, Nucl. Phys. **B339** (1990) 222.

FIGURES

$$\begin{aligned}
 G_{\pi\pi \rightarrow \pi\pi}(t) = & \begin{array}{c} \text{-p} \quad \text{0} \\ \updownarrow \quad \updownarrow \\ \text{p} \quad \text{0} \end{array} - \begin{array}{c} \diagup \quad \diagdown \\ \diagdown \quad \diagup \end{array} + \begin{array}{c} \leftarrow \quad \leftarrow \\ \rightarrow \quad \rightarrow \end{array} + \begin{array}{c} \rightarrow \quad \rightarrow \\ \leftarrow \quad \leftarrow \end{array} - \begin{array}{c} \rightarrow \quad \rightarrow \\ \leftarrow \quad \leftarrow \end{array} - \begin{array}{c} \rightarrow \quad \rightarrow \\ \leftarrow \quad \leftarrow \end{array} \\
 G_{\pi\pi \rightarrow \rho}(t) = & \begin{array}{c} \text{-p} \\ \diagdown \quad \diagup \\ \text{p} \quad \text{0} \end{array} - \begin{array}{c} \diagdown \quad \diagup \\ \diagup \quad \diagdown \end{array} \qquad G_{\rho \rightarrow \pi\pi}(t) = \begin{array}{c} \text{-p} \quad \text{0} \\ \rightarrow \quad \rightarrow \\ \text{p} \end{array} - \begin{array}{c} \leftarrow \quad \leftarrow \\ \diagdown \quad \diagup \end{array}
 \end{aligned}$$

FIG. 1: Quark contractions of $\pi\pi \rightarrow \pi\pi$, $\pi\pi \rightarrow \rho$ and $\rho \rightarrow \pi\pi$ components of the time correlation function $G(t)$. Vertices refer to the pion or the ρ meson with a momentum specified in the diagram. The time runs upward in the diagrams.

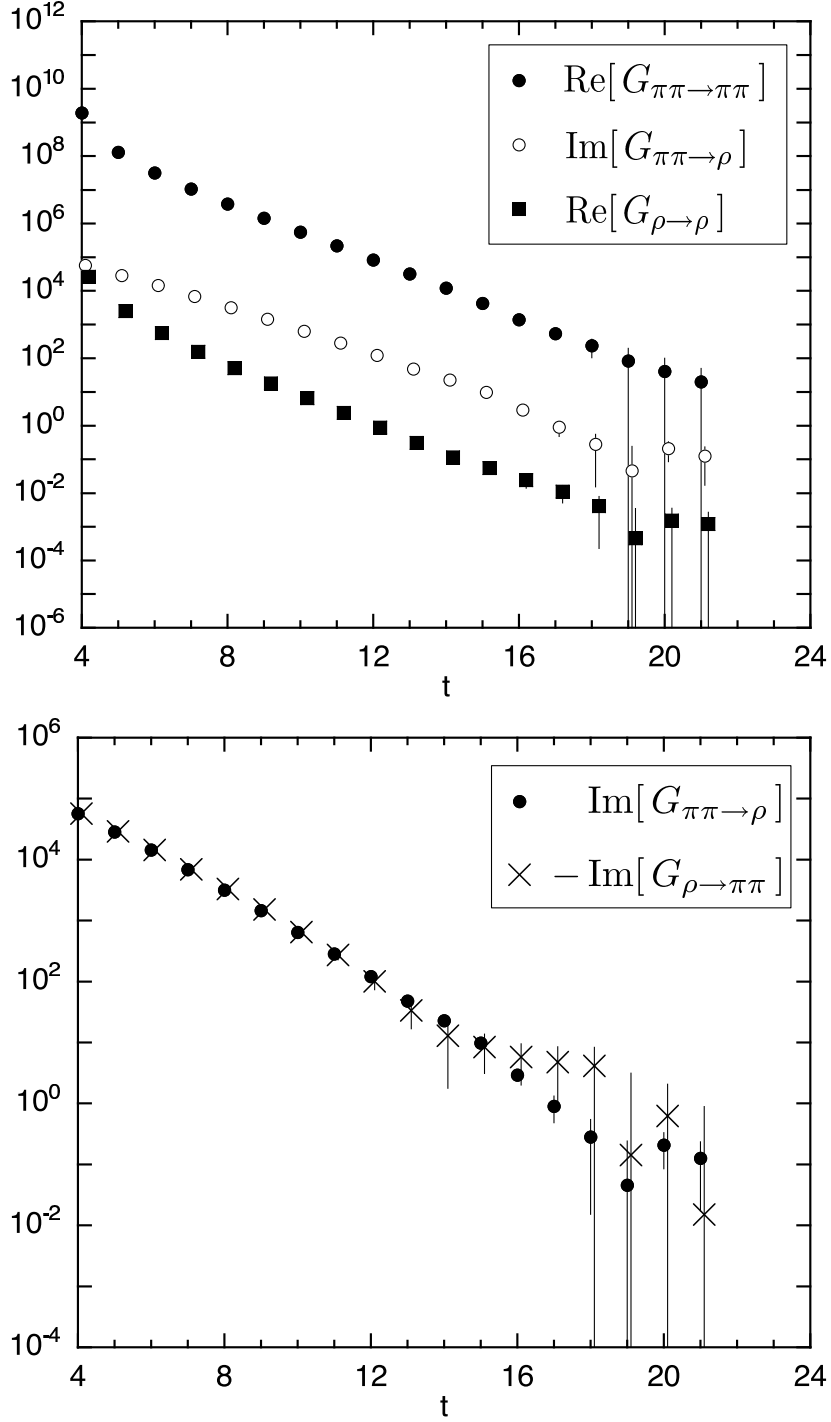


FIG. 2: Real part of the diagonal components ($\pi\pi \rightarrow \pi\pi$ and $\rho \rightarrow \rho$) and the imaginary part of the off-diagonal components ($\pi\pi \rightarrow \rho$ and $\rho \rightarrow \pi\pi$) of the time correlation function $G(t)$.

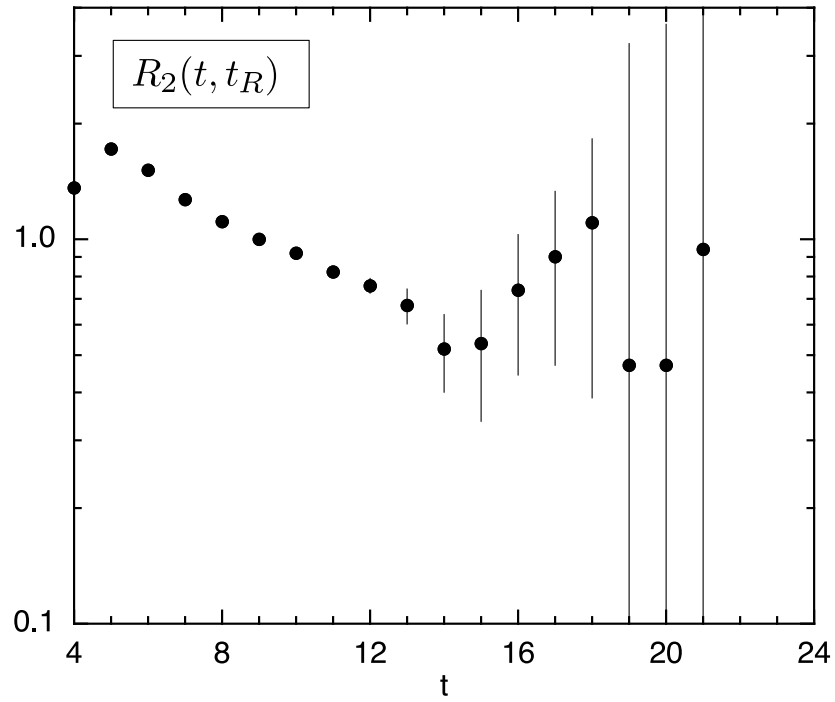
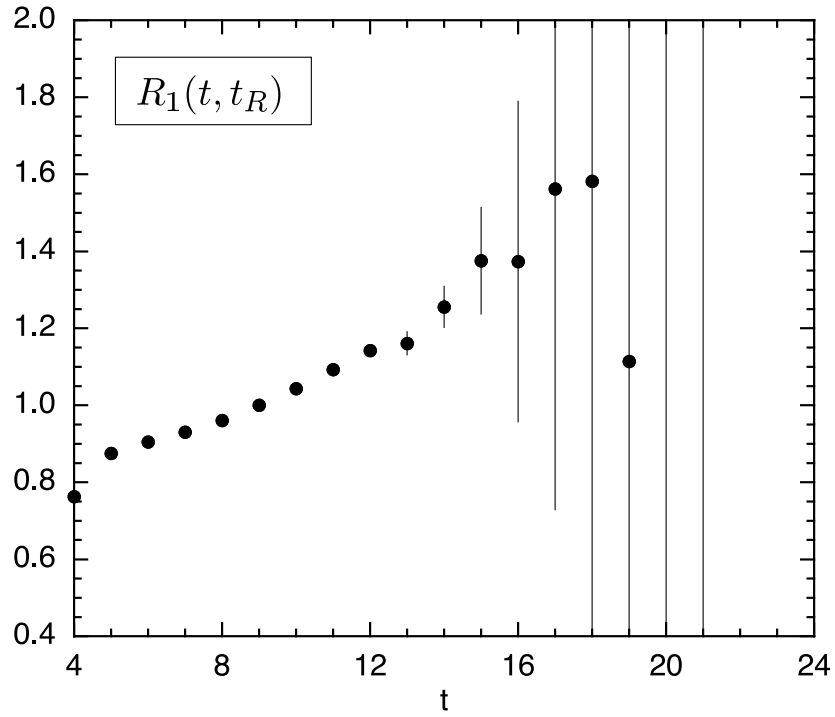


FIG. 3: Normalized eigenvalues $R_1(t, t_R)$ and $R_2(t, t_R)$.

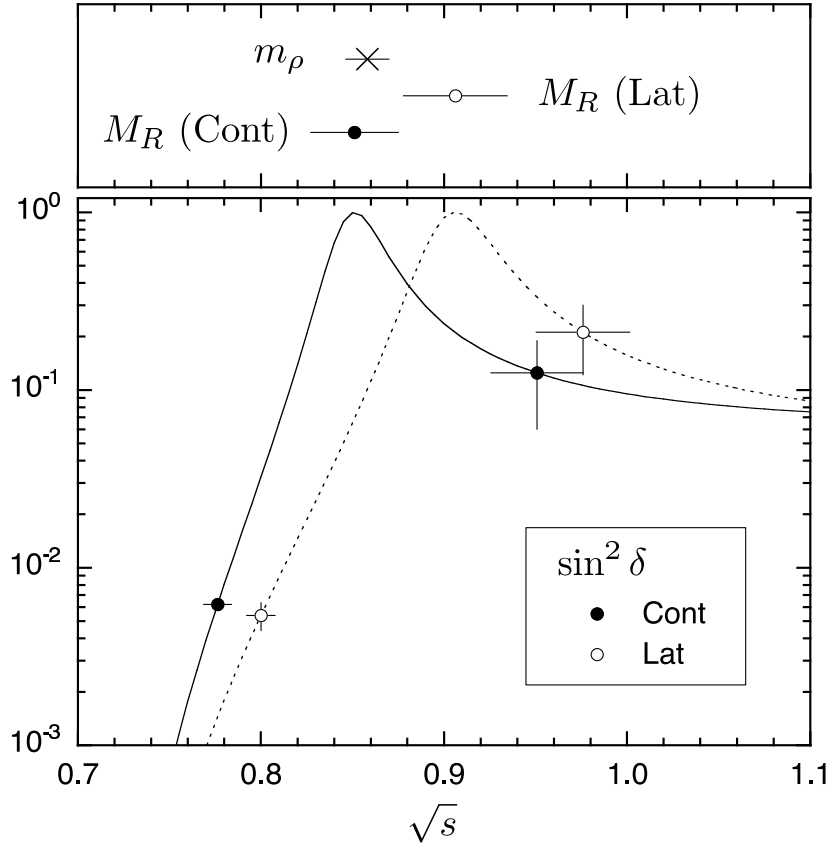


FIG. 4: Scattering phase shift $\sin^2 \delta$ (lower panel), positions of m_ρ and resonance mass M_R (upper panel). **Cont** refer to the results obtained with the energy-momentum relations in the continuum (24) and **Lat** to those with the relations on the lattice (26). The two lines are given by (27) with parameters $g_{\rho\pi\pi}$ and M_R given in (29) and (30). The abscissa is in lattice units.

TABLES

	$n = 1$		$n = 2$	
W_n^0	0.9805(51)		—	
ΔW_n	−0.0441(60)		0.105(22)	
W_n	0.9364(63)		1.085(22)	
	Cont	Lat	Cont	Lat
\sqrt{s}	0.7764(76)	0.8000(77)	0.951(25)	0.976(26)
k^2	0.0235(26)	0.0337(28)	0.099(12)	0.115(13)
k_0^2	—	0.0328(27)	—	0.111(12)
$\tan \delta$	0.07906(93)	0.0736(66)	−0.38(11)	−0.52(14)
$\sin^2 \delta$	0.00621(14)	0.00539(96)	0.125(65)	0.211(90)

TABLE I: Energy of the two-pion system W_n and the scattering phase shift δ . W_1^0 is the energy of the two free pions. W_n is reconstructed from the energy difference ΔW_n by $W_n = \Delta W_n + W_1^0$. The invariant mass \sqrt{s} , the the momentum k and the phase shifts δ calculated with the energy-momentum relations in the continuum (24) are referred to as **Cont**, and those obtained with the relations on the lattice (26) are referred to as **Lat**. The momentum k_0 is defined by $k_0^2 = s/4 - m_\pi^2$. All values with the mass dimension are in units of the lattice spacing.

	π		ρ	
m	0.3567(24)		0.858(12)	
E	0.6238(38)		1.019(27)	
	Cont	Lat	Cont	Lat
p_{eff}^2	0.2620(45)	0.2799(50)	0.301(59)	0.358(74)
p_{eff}^2/p^2	0.956(16)	1.021(18)	1.10(22)	1.31(27)

TABLE II: Mass m and energy E of the pion and the ρ meson with the momentum $\mathbf{p} = p\mathbf{e}_3 = (2\pi/L)\mathbf{e}_3$, extracted from the time correlation function. The momenta p_{eff} calculated from the dispersion relation in the continuum (22) are referred to as **Cont** and that from the relation on the lattice (23) as **Lat**. All values are in units of the lattice spacing.